fact, the P═P π bond is about as strong as the Si═C bond, in spite of the fact that silaethylene contains only one third-row atom.

Borden and co-workers[61] have offered a simple explanation of the difference between P and Si multiple bonding, in terms of so-called "inert-pair effect". Atoms in the third row are reluctant to form sp hybrids, leading to preferred bond angles near 90°. To form a π bond Si must hybridize, giving up its predominantly s lone pair, whereas P need not.

trans-HPPH is found to be more stable than the H_2PP isomers by around 27 kcal/mol. The lowest energy unimolecular process converting *trans*- to *cis*-HPPH is rotation about the π bond, in contrast to the inversion mechanism for HNNH.[17] H_2PP has two quite closely spaced states, a bent triplet and a planar, doubly bonded singlet. Confident prediction of the ground state of phosphinophosphinidene must therefore await the experimental demonstration of such a compound.

The hydrogenation of diphosphene to diphosphine is computed to be exothermic by 25 kcal/mol, in good agreement with the experimental estimate of 21 ± 8 kcal/mol.[7] The concerted hydrogenation has a quite substantial barrier (about 63 kcal/mol) and proceeds via an initially one-sided attack. Pyrolysis of the saturated diphosphine has a lower barrier for 1,1-elimination to H_2PP than 1,2-elimination to HP═PH (67 vs. 87 kcal/mol). (We have not considered other possible channels, such as H + $HPPH_2$, or PH + PH_3.)

Acknowledgment. Computer time for this work was provided by the North Dakota State University Computer Center. This work was supported by AFOSR Grant 82-0190.

Registry No. HP═PH, 41916-72-7; H_2P═P, 90883-63-9; HP═NH, 61559-67-9; HN═NH, 3618-05-1.

---

(61) (a) Feller, D.; Davidson, E. R.; Borden, W. T. *J. Am. Chem. Soc.* **1985**, *107*, 2596-2597. (b) Cherry, W.; Epiotis, N.; Borden, W. T. *Acc. Chem. Res.* **1977**, *10*, 167-173.

Contribution from the Instituto de Física e Química de São Carlos, University of São Paulo, 13560 São Carlos, SP Brazil, and Department of Chemistry, University of Calgary, Calgary, Alberta, Canada T2N 1N4

Structure and Properties of the Sulfur Dinitride Dianion

M. Conti,[†] M. Trsic,[†] and W. G. Laidlaw*[‡]

Received March 4, 1985

The properties of the N_2S^{2-} dianion are calculated by using Hartree–Fock–Slater and MNDO methods and are related to those of N_2S and experimental results. A locally stable NSN^{2-} species with an NSN angle of 135° is characterized, and a decomposition channel to N_2 + S^{2-} is identified.

I. Introduction

A C_{2v} form of the sulfur dinitride fragment, NSN, appears to be transferred in various reactions encountered in sulfur nitride chemistry.[1,2] This motivated us recently to report a Hartree–Fock–Slater (HFS) MO–LCAO[3] calculation for the N_2S species.[1] While the linear NNS form appeared to be the ground state of the molecule, we were abe to detect a local minimum for a symmetric species with an NSN angle of 90° (NSN-90), with a barrier of some 9–15 kcal/mol toward decomposition into N_2 + S. However, the symmetrical NSN species has not been isolated so far. Nevertheless, the N_2S^{2-} dianion has been obtained recently by two different routes.[4,5]

The crystal structure of N_2S^{2-} is not known, but on the basis of vibrational spectra[4] there seems to be no doubt that it has a symmetrical NSN form. It seems interesting to complete our calculations on the NSN fragment by reporting features for the dianion of this species. We focus on the geometrical structure, the UV spectrum, and the electronic structure and relate our findings to the neutral NSN fragment and to experimental results.

II. The NSN Fragment

It is useful to start by recalling briefly the main features of the electronic structure of NSN and relate them to the NSN^{2-} anion. The NSN-90 fragment single determinant valence orbital configuration is $a_1{}^8a_2{}^2b_1{}^2b_2{}^4$ with four π electrons (a_2 and b_1). The lowest unoccupied MO (LUMO), $3b_2$, is a σ orbital with moderate SN bonding character and very strong NN antibonding behavior. Thus, the occupancy of this orbital to form a dianion should strengthen somewhat the SN bonds and open the NSN angle. At NSN angles of ≤60° there is a decomposition channel leading to the formation of N_2 and S. The configuration of the wave function for this species is $a_1{}^8a_2{}^{20}b_1{}^4b_2{}^4$ where the a_2 orbital, which is NS bonding and NN antibonding, is now empty while $2b_1$, an antibonding, π^*_{NS} orbital, is occupied with the result that the NS bond is weakened and the NN linkage strengthened through the $1a_2 \rightarrow 2b_1$ electron transfer.

As remarked earlier, the absolute minimum for the N_2S species is a linear NNS form, and this too can be analyzed as to the effect of adding two electrons. The LUMO of linear NNS is a π orbital with antibonding NN character and little NS bonding. The addition of two electrons to this orbital would certainly weaken the overall bonding. Furthermore, since this orbital is degenerate, the linear NNS^{2-} anion is unlikely to be stable.

III. The NSN^{2-} Anion

III.1. Geometry. As a first step for the geometry optimization of the NSN^{2-} anion we employed the MNDO program, which is well suited for this purpose.[6,7] Keeping the SN distance fixed at 1.6 Å and letting the NSN angle vary up to 180°, one can locate a minimum for the standard heat of formation, $\Delta H_f°$, between 110 and 120° (Figure 1). A full optimization in this region leads to an NSN angle of 118° and a SN distance of 1.53 Å. At low angles $\Delta H_f°$ decreases steadily indicating a decomposition channel just as in NSN and leading, in this case, to N_2 + S^{2-} with a barrier toward decomposition of ca. 25 kcal/mol.

As for the HFS method, the total statistical energy, E_T, indicates a very flat minimum for an NSN angle around 135°, NSN-135(2−) (Figure 2), with the NS distance fixed at 1.6 Å. Further variation of the NS distance indicates a minimum for 1.60 Å. Again, for small angles, there appears to be a decomposition channel (cf. Figure 2).

III.2. Electronic Structure of the NSN-135(2−) Anion. In the following sections we provide a description of the electronic structure of NSN(2−) based on the HFS results for an NSN angle

---

[†] University of São Paulo.

[‡] University of Calgary.

(1) Laidlaw, W. G.; Trsic, M. *Inorg. Chem.* **1981**, *20*, 1792.
(2) Chivers, T.; Laidlaw, W. G.; Oakley, R. T.; Trsic, M. *J. Am. Chem. Soc.* **1980**, *102*, 5773.
(3) Baerends, E. J.; Ros, P. *Int. J. Quantum Chem. Symp.* **1978**, *12*, 169.
(4) Herberhold, M.; Ehrenreich, W. *Angew. Chem., Int. Ed. Engl.* **1982**, *21*, 633.
(5) Chivers, T.; Hojo, M. *Inorg. Chem.* **1984**, *23*, 1526.
(6) Dewar, M. J. S.; Thiel, W. *J. Am. Chem. Soc.* **1977**, *99*, 4899.
(7) Dewar, M. J. S.; McKee, M. L. *J. Comput. Chem.* **1983**, *4*, 84.

0020-1669/86/1325-0254$01.50/0

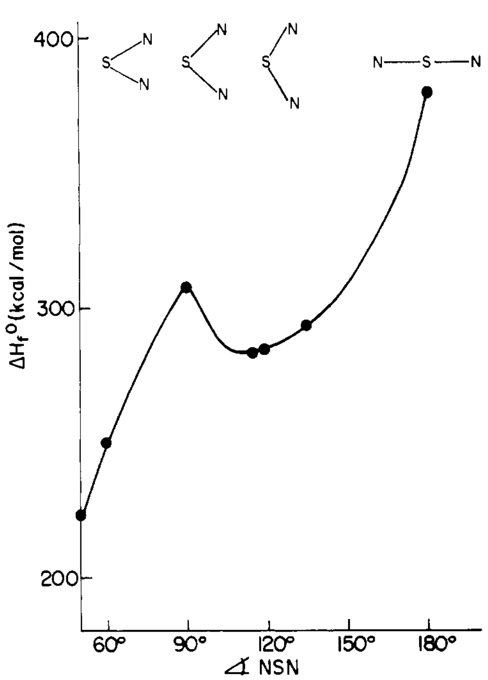

Figure 1. Variation of the standard heat of formation, $\Delta H_f°$, with the NSN angle in the NSN(2-) anion as provided by the MNDO method. The SN distance is fixed at 1.6 Å.

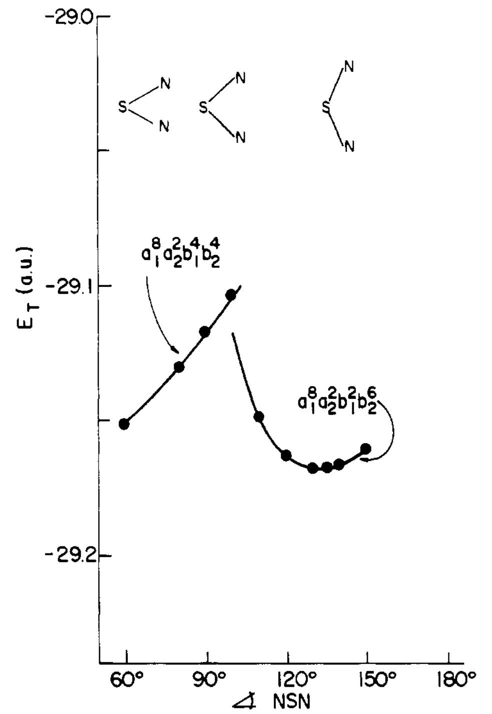

Figure 2. Total statistical energy, E_T, as a function of the NSN angle in NSN(2-). The SN distance is fixed at 1.6 Å.

of 135° and SN distance of 1.60 Å.

III.2.1. Bonding Properties of the MO's. The configurational of the ground state of NSN-135(2-) is $a_1^8a_2^2b_1^2b_2^6$. Other than the fact that the NN interactions are of less concern for the geometry of the anion, the characteristics of the MO's of NS-N-135(2-) are, to a large extent, the same as for NSN-90. Some differences can be noted however; for example, in the lower part of the stack $3a_1$ and in the frontier region $4a_1$ and the newly occupied $3b_2$ orbital are all altered somewhat. Indeed, the antibonding $3a_1$ orbital of the neutral species becomes NS bonding in the anion whereas $3b_2$, which is moderately bonding in NSN-90, acquires more bonding character when occupied. On the other hand, the lone pair type orbital $4a_1$ of NSN-90 adds some antibonding character in the ion. As a result of the trend in the above orbitals one expects a slight enhancement of the overall SN bond strength, which does happen (see section III.2.2). In general terms, the ground state of NSN-135(2-) may be described as $\sigma^8(\sigma^*)^6\pi^4$, which leaves, on balance, one σ and two π occupied bonding orbitals.

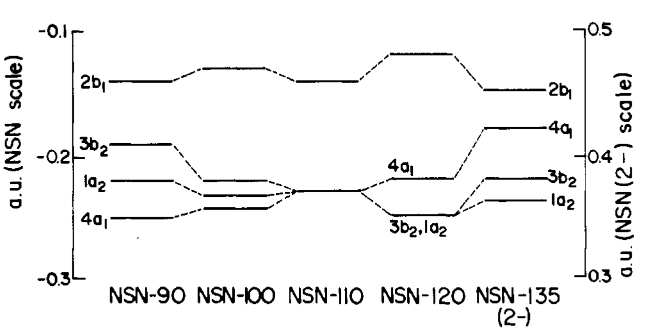

Figure 3. Correlation diagram for the frontier orbitals of NSN-135(2-) and NSN at various angles.

III.2.2. Overall Electron Density Distribution. The charges in NSN-135(2-) are -0.85 on N and -0.30 on S. Comparison of these values with charges in NSN-90 (-0.015 and -0.30, respectively) implies that the two extra electrons are evenly distributed among the three centers.

The Mulliken atom-atom SN overlap population of 0.47 indicates a single bond, somewhat stronger than in NSN-90. The splitting of the overlap population into the σ and the π systems indicates a 0.37 π contribution and a 0.11 σ contribution. The corresponding values for NSN-90 are of 0.28 π and 0.13 σ. Consequently, one can describe NSN-135(2-) as primarily linked by π bonds resulting fom four π electrons distributed over the three centers, i.e., two electrons per linkage.

III.2.3. Eigenvalues and Electronic Transitions. While the two extra electrons of the anion may be considered as going into the LUMO of NSN-90, i.e., $3b_2$, this orbital does not remain as the highest occupied MO (HOMO) of the anion but is pushed down in the stack and $4a_1$ becomes the HOMO. In order to determine whether the orbital reorganization is a result of the addition of the two electrons or of the change in geometry, we have followed the behavior of the frontier orbitals of NSN as one goes from an NSN angle of 90° to 120° in steps of 10° (Figure 3). It is actually $4a_1$, HOMO-1 in NSN-90, which becomes HOMO in NSN-135(2-). As Figure 3 indicates, a change in geometry will, of itself, cause the necessary reorganization of orbitals (the crossing occurs at an angle of 110°).

The lowest allowed transitions in NSN-135(2-) are $4a_1 \rightarrow 2b_1$ ($\sigma \rightarrow \pi$) and $1a_2 \rightarrow 2b_1$ ($\pi \rightarrow \pi^*$). We have calculated the wavelengths of both transitions with Slater's transition-state method[8] and the HFS function. The value for $4a_1 \rightarrow 2b_1$ is 470 nm whereas the $\pi \rightarrow \pi^*$ transition is calculated to be at 340 nm. Both these values are at variance with the experimental λ_{max} of 253 nm.[5] In this connection it is worth noting that the $4a_1 \rightarrow 2b_1$ ($n \rightarrow \pi^*$) transition in ozone corresponds to the weak band at 600 nm, not to the strong characteristic 250-nm band.[9] The latter involves rather more complex rearrangement of orbital occupancy in ozone,[10] and such may also be the case in N_2S^{2-}. Indeed, using the same scheme as for ozone[10] for the $4a_1$ and $2b_1$ orbitals gives, for the 120° conformation, a value of 236 nm for λ_{max} whereas for the 135° conformation one obtains λ_{max} 312 nm, the two values bracketing the experimental value of 253 nm.

IV. The NNS^{2-} Anion

As anticipated (section II), the linear NNS^{2-} anion appears to be a triplet. The MNDO-calculated value for $\Delta H_f°$ is ca. 100 kcal/mol lower for the triplet than for the singlet at this geometry.

---

[8] Slater, J. C. *Adv. Quantum Chem.* **1972**, *6*, 1.

[9] Hay, P. J.; Dunning, T. H.; Goddard, W. A. *J. Chem. Phys.* **1975**, *62*, 3912.

[10] Rearrangements involving transitions such as $(4a_1)^2(2b_1)^0 \rightarrow (4a_1)^0(2b_1)^2$ have been cited (see ref 9 section C) as contributing to the band in ozone.

This triplet is not a minimum in the energy-geometry surface but is on a decomposition channel toward $S^{2-} + N_2$. We could locate a minimum for a singlet bent form of NNS^{2-} with an NNS angle of 120° and NN and NS distances of 1.17 and 1.72 Å, respectively. This bent NNS^{2-} conformation is some 150 kcal/mol below the symmetric bent NSN^{2-} anion described in the previous section. Nevertheless, an HFS analysis of the bonding in this bent NNS^{2-} singlet indicates an unstable species. Indeed, the atom-atom overlap populations show a strong NS antibonding interaction and little NN bonding. Further this state is crossed by the triplet decomposition channel leading to S^{2-} and N_2 mentioned above. Thus the NNS^{2-} bent form would be unstable through intersystem crossing to the unbound triplet state.

V. Conclusions

The stability of the symmetric N_2S^{2-} species relative to that of the apparently elusive symmetric N_2S reaction fragment is not too surprising. Both the NS bond and the barrier to decomposition are considerably stronger in the dianion. We find $p_{NS}(2-) = 0.47$ vs. $p_{NS} = 0.41$ and $\Delta H_{dec}(2-) = 25$–30 kcal/mol vs. $\Delta H_{dec} = 9$–15 kcal/mol. Not surprisingly, the dianion can be considered as the reduction product of N_2S. The changes in structure, such as angle opening, and orbital energies are primarily those expected on addition of two electrons to N_2S. As in the case of the isoelectronic species, ozone, the UV band at 253 nm likely corresponds to a more complex transition than just a single excitation $4a_1 \rightarrow 2b_1$.

Contrary to the case of the neutral N_2S species, which has an asymmetric linear ground state, the asymmetric form of the dianion, according to our results, is unstable toward decomposition into $S^{2-} + N_2$.

Acknowledgment. This work was supported by NSERC/Canada and CNPq/Brazil grants. M.C. is grateful for a CNPq Fellowship. We thank T. Chivers for bringing this problem to our attention.

Registry No. N_2S^{2-}, 79796-15-9.

Contribution from the Istituto Chimico "G. Ciamician" and Istituto FRAE-CNR, Bologna, Italy,
and Institute of Inorganic Chemistry, University of Fribourg, Fribourg, Switzerland

Excited-State Properties of Ruthenium(II) Tris Chelate Complexes Containing the Ligands 2,2′-Bipyridine (bpy) and Dipyrido[3,2-*c*:2′,3′-*e*]pyridazine (taphen)

Alberto Juris,[1a,b] Peter Belser,[1c] Francesco Barigelletti,[1b] Alex von Zelewsky,[1c] and Vincenzo Balzani*[1a,b]

Received March 25, 1985

The complexes $Ru(bpy)_{3-n}(taphen)_n^{2+}$ (n = 0–3, bpy = 2,2′-bipyridine, taphen = dipyrido[3,2-*c*:2′,3′-*e*]pyridazine) have been prepared, and their absorption spectra, emission spectra, emission lifetimes, luminescence quantum yields, and redox potentials have been measured. The first reduction potential of the three taphen-containing complexes is almost the same as (~ −0.72 V vs. SCE) and much less negative than that of $Ru(bpy)_3^{2+}$ (−1.35 V). The first oxidation potential increases by 0.11 V as each bpy of $Ru(bpy)_3^{2+}$ is replaced by taphen. The maximum of the metal-to-ligand charge-transfer (MLCT) absorption band of the taphen-containing complexes lies at slightly higher energy than that of $Ru(bpy)_3^{2+}$, while the emission maximum lies at lower energy. The lifetime of the emitting excited state is in the 1-μs range at 77 K and in the 0.1-μs range at room temperature, as expected for formally triplet MLCT excited states. $Ru(taphen)_3^{2+}$ does not follow the correlation observed by other RuL_3^{2+} complexes between energy of the absorption maximum and $[E_{1/2}(RuL_3^{3+/2+}) - E_{1/2}(RuL_3^{2+/+})]$, showing that different π^*(taphen) orbitals are involved in the two processes. Examination of the analogous correlation involving the emission maxima shows that the π^*(taphen) orbital involved in reduction is presumably the same as that involved in the luminescence emission. A possible explanation for this behavior lies on the inverted energy ordering of the π^* ψ and χ orbitals in taphen compared with that found for α,α'-diimines. At 77 K the excited-state lifetime of $Ru(bpy)_{3-n}(taphen)_n^{2+}$ seems to be governed by the energy gap law. The shorter lifetimes of the complexes containing taphen at room temperature should not result from deactivation via ^{3}MC since the energy gap between the luminescent ^{3}MLCT levels and the upper lying ^{3}MC level is expected to be larger than in $Ru(bpy)_3^{2+}$.

Introduction

After the discovery[2,3] of the extremely interesting photochemical and photophysical properties of $Ru(bpy)_3^{2+}$ (bpy = 2,2′-bipyridine),[4-8] a number of analogous Ru complexes have been prepared to obtain a better understanding of the metal-ligand and ligand-ligand interactions and to tune the excited-state properties in a controlled manner.[9-18] Continuing our studies in this field, we have synthetised a new family of Ru(II) complexes that contain the quite interesting taphen ligand (taphen = dipyrido[3,2-*c*:2′,3′-*e*]pyridazine, Figure 1). We report here results concerning a spectroscopic, photophysical, and electrochemical investigation of the $Ru(bpy)_{3-n}(taphen)_n^{2+}$ complexes (n = 0–3) and a comparative discussion of the observed properties.

Experimental Section

$Ru(bpy)_3^{2+}$, $Ru(bpy)_2(taphen)^{2+}$, $Ru(bpy)(taphen)_2^{2+}$, and $Ru(taphen)_3^{2+}$ as PF_6^- salts were prepared and purified by following a procedure previously described.[19] The synthesis of taphen will be reported elsewhere.[20] The solvents used were acetonitrile or ethanol–methanol

---

(1) (a) Istituto Chimico "G. Ciamician". (b) Istituto FRAE-CNR. (c) University of Fribourg.

(2) Gafney, D. H.; Adamson, A. W. *J. Am. Chem. Soc.* **1972**, *94*, 8238.

(3) Crosby, G. A. *Acc. Chem. Res.* **1975**, *8*, 231.

(4) Balzani, V.; Bolletta, F.; Gandolfi, M. T.; Maestri, M. *Top. Curr. Chem.* **1978**, *75*, 1.

(5) DeArmond, M. K.; Carlin, C. M. *Coord. Chem. Rev.* **1981**, *36*, 325.

(6) Kalyanasundaram, K. *Coord. Chem. Rev.* **1982**, *46*, 159.

(7) Balzani, V.; Bolletta, F.; Ciano, M.; Maestri, M. *J. Chem. Educ.* **1983**, *60*, 447.

(8) Watts, R. J.; *J. Chem. Educ.* **1983**, *60*, 834.

(9) The literature in this field is very rich. Most of the previous papers are quoted in the recent references 10–18.

(10) Rillema, D. P.; Allen, G.; Meyer, T. J.; Conrad, D. *Inorg. Chem.* **1983**, *22*, 1617.

(11) Crutchley, R. J.; Kress, N.; Lever, A. B. P. *J. Am. Chem. Soc.* **1983**, *105*, 1170.

(12) Kitamura, N.; Kawanishi, Y.; Tazuke, S. *Chem. Phys. Lett.* **1983**, *97*, 103.

(13) Allen, G. H.; White, R. P.; Rillema, D. P.; Meyer, T. J. *J. Am. Chem. Soc.* **1984**, *106*, 2613.

(14) Cherry, W. R.; Henderson, L. J. Jr. *Inorg. Chem.* **1984**, *23*, 983.

(15) Morris, D. E.; Ohsawa, Y.; Segers, D. P.; DeArmond, M. K.; Hanck, K. W. *Inorg. Chem.* **1984**, *23*, 3010.

(16) Ackermann, M. N.; Interrante, L. V. *Inorg. Chem.* **1984**, *23*, 3904.

(17) Juris, A.; Barigelletti, F.; Balzani, V.; Belser, P.; von Zelewsky, A. *Inorg. Chem.* **1985**, *24*, 202.

(18) Balzani, V.; Juris, A.; Barigelletti, F.; Belser, P.; von Zelewsky, A. *Riken Q.* **1984**, *78*, 78.

(19) Belser, P.; von Zelewsky, A. *Helv. Chim. Acta* **1980**, *63*, 1675.

(20) Belser, P., submitted for publication.